

Leveraging Synthetic Priors for Monocular Depth Estimation in Specular Surgical Environments

Ankan Aich¹ and Yangming Lee¹

¹RoCAL, Rochester Institute of Technology, Rochester, NY, USA, 14456
{aa5365, ymliee}@rit.edu

Abstract—Accurate Monocular Depth Estimation (MDE) is critical for robotic surgery but remains fragile in specular, fluid-filled endoscopic environments. Existing self-supervised methods, typically relying on foundation models trained with noisy real-world pseudo-labels, often suffer from boundary collapse on thin surgical tools and transparent surfaces. In this work, we address this by leveraging the high-fidelity synthetic priors of the *Depth Anything V2* architecture, which inherently captures precise geometric details of thin structures. We efficiently adapt these priors to the medical domain using Dynamic Vector Low-Rank Adaptation (DV-LORA), minimizing the parameter budget while bridging the synthetic-to-real gap. Additionally, we introduce a physically-stratified evaluation protocol on the SCARED dataset to rigorously quantify performance in high-specularity regimes often masked by aggregate metrics. Our approach establishes a new state-of-the-art, achieving an accuracy ($\delta < 1.25$) of 98.1% and reducing Squared Relative Error by over 17% compared to established baselines, demonstrating superior robustness in adverse surgical lighting.

Index Terms—Monocular Depth Estimation; Foundation Models; Synthetic-to-Real Adaptation; Autonomous Robotic Surgery

I. INTRODUCTION

A. 3D Perception in Robotic Surgery

Precise 3D dense reconstruction is a fundamental requirement for the advancement of autonomous robotic surgery. Beyond simple visualization, depth estimation serves as the geometric foundation for critical downstream tasks, including dynamic active constraints, intraoperative registration, soft tissue tracking, and augmented reality overlay [1]–[4]. In these safety-critical applications, the perception system must deliver robust geometric information from monocular endoscopic video in real-time, enabling the robotic agent to interact safely with the complex anatomy of the patient [5]–[7].

B. Challenges in the Surgical Domain

Despite its importance, robust depth estimation in Minimally Invasive Surgery (MIS) remains a formidable challenge due to the unique and hostile nature of the endoscopic environment. As comprehensively reviewed in [8], surgical scenes violate nearly all photometric assumptions used in standard computer vision. The environment is characterized by homogeneous tissue textures, rapid non-rigid deformations caused by respiration or instrument interaction [9]–[11], and severe non-Lambertian effects—specifically, high-intensity specular reflections on wet surfaces and transparent

fluids [12], [13]. Furthermore, unlike autonomous driving or indoor navigation, the surgical domain suffers from a critical scarcity of reliable ground truth data. Active sensors (e.g., structured light) frequently fail due to signal saturation in specular regions, making it difficult to train fully supervised models that generalize across different patients and procedures [14], [15].

C. The Evolution of Vision Backbones

In the broader computer vision and robotics community, the landscape of dense prediction has been revolutionized by several paradigm shifts. The introduction of Vision Transformers (ViTs) shifted feature extraction from local convolutions to global attention mechanisms, enabling models to capture long-range dependencies [16]. Simultaneously, Neural Radiance Fields (NeRFs) and Gaussian Splatting have transformed 3D representation, offering photorealistic reconstruction from sparse views [17], [18]. Generative approaches, such as Diffusion Models, have also shown remarkable capability in hallucinating missing geometric details [19]. Most notably, the rise of “Foundation Models”—such as the Segment Anything Model (SAM) [20] and the Depth Anything series [21]—has demonstrated that models trained on massive-scale, diverse datasets can achieve unprecedented zero-shot generalization.

However, adapting these general-purpose breakthroughs to the surgical domain presents a significant bottleneck. NeRF and diffusion-based methods often entail prohibitive computational costs or latency incompatible with real-time surgical feedback [22]. Foundation models, while powerful, are predominantly trained on “natural” imagery (e.g., street scenes, indoor objects). When applied directly to endoscopic footage, these models suffer from a severe domain shift. The geometric priors learned from natural scenes often fail to resolve the fine-grained boundaries of thin surgical tools or distinguish between transparent fluids and tissue surfaces, leading to artifacts that compromise safety.

D. Bridging the Gap: Synthetic Priors and Efficient Adaptation

To address these limitations, we propose a framework that bridges the gap between state-of-the-art general vision models and the specific constraints of robotic surgery. Rather than training a model from scratch on limited medical data, or blindly applying a generalist model, we leverage the specific

strengths of the *Depth Anything V2* (DAv2) architecture [23]. Unlike its predecessors trained on noisy real-world data [24], DAv2 is pre-trained on high-fidelity **synthetic** environments. We identify that these "synthetic priors" are uniquely suited for surgery, as they inherently capture the sharp geometric boundaries of thin structures and transparent objects often lost in real-world training. We adapt these priors to the medical domain using parameter-efficient Dynamic Vector Low-Rank Adaptation (DV-LORA), allowing us to fine-tune the model for surgical textures without destroying its robust structural understanding.

E. Contributions

Our main contributions are summarized as follows:

- 1) We propose a robust adaptation framework that successfully transfers the synthetic priors of foundation models to the endoscopic domain, addressing the specific problem of boundary collapse in thin tools and fluids.
- 2) We demonstrate that by integrating DV-LORA with the DAv2 backbone, we achieve state-of-the-art reconstruction performance with a minimal trainable parameter budget.
- 3) Addressing the evaluation gap noted in [8], we introduce a **physically-stratified evaluation protocol** on the SCARED dataset [14]. By clustering frames based on sensor failure rates, we rigorously quantify robustness in high-specularity regimes, demonstrating significant improvements over baselines trained on real-world priors.

II. RELATED WORKS

A. Self-Supervised Depth Estimation in Surgery

Traditional self-supervised methods, pioneered by SfM-Learner and Monodepth2 [25], rely on photometric consistency to learn depth without ground truth. In the medical domain, numerous works have adapted this paradigm to endoscopy [15]. Recently, Cui et al. introduced **EndoDAC** [24], a state-of-the-art framework that successfully adapted large-scale foundation models to the surgical domain using Parameter-Efficient Fine-Tuning (PEFT). Their work demonstrated that freezing a pre-trained backbone and injecting lightweight Dynamic Vector LoRA (DV-LORA) modules could achieve superior robustness compared to training from scratch. Our work builds directly upon this efficient adaptation architecture.

B. Foundation Models: Real vs. Synthetic Priors

The core differentiator of modern depth estimation is the pre-training data. The *Depth Anything V1* backbone, utilized in the original EndoDAC, was trained using a semi-supervised pipeline on massive real-world datasets. While effective for general scenes, recent analyses suggest that V1's reliance on pseudo-labels introduces "label noise" around thin structures and transparent surfaces, as the teacher model often hallucinates in these regions [23].

To address this, the recently introduced *Depth Anything V2* (DAv2) shifts the training paradigm to high-fidelity **synthetic**

environments [23]. This "synthetic prior" provides mathematically precise supervision for challenging optical properties (transparency, reflections) that are ubiquitous in surgery but noisy in real-world data. In this paper, we extend the EndoDAC framework by replacing the V1 backbone with DAv2, effectively combining Cui et al.'s efficient adaptation strategy with the superior geometric priors of synthetic pre-training.

III. METHODOLOGY

A. Framework Overview

Our framework builds upon the parameter-efficient adaptation strategy introduced in EndoDAC [24], redesigning it to leverage the synthetic-to-real generalization capabilities of the *Depth Anything V2* (DAv2) architecture. The pipeline consists of two primary components: a **DepthNet**, which predicts dense depth maps from single frames, and a **Pose-Intrinsics Net**, which estimates the 6-DoF camera motion and focal length to enable self-supervised training on uncalibrated video.

B. DepthNet: Injecting Synthetic Priors

The core innovation of our approach is the integration of the DAv2 backbone to solve the specific challenge of boundary collapse in endoscopic footage.

1) *Backbone Selection and Freezing*: Unlike previous iterations relying on real-world supervision, we utilize the DAv2 encoder pre-trained on high-fidelity synthetic data. This initialization provides the network with robust "synthetic priors"—specifically, the ability to resolve thin geometric structures and transparent surfaces, which are mathematically precise in synthetic training sets but noisy in real-world pseudo-labels. To preserve these priors, we **freeze** the entire transformer backbone during training. This ensures that the model's fundamental understanding of object boundaries is not catastrophically forgotten during the adaptation to medical textures.

2) *Dynamic Vector Adaptation (DV-LORA)*: To adapt the frozen synthetic features to the specific photometric domain of endoscopy (e.g., wet tissue, blood), we inject trainable Dynamic Vector LoRA (DV-LORA) modules into the attention layers. Unlike standard LoRA, which uses static low-rank matrices, DV-LORA introduces dynamic vectors that scale the feature projection, allowing the model to capture the high dynamic range of surgical lighting with minimal parameters. The updated weight matrix \hat{W} is defined as:

$$\hat{W} = W_0 + \Lambda_v B \Lambda_u A, \quad (1)$$

where W_0 is the frozen pre-trained weight, A and B are low-rank matrices, and Λ_u, Λ_v are diagonal matrices containing the learnable dynamic vectors. This configuration adds only $\approx 1.6M$ trainable parameters to the massive DAv2 backbone.

3) *High-Frequency Restoration*: Vision Transformers often act as low-pass filters, smoothing out fine texture details crucial for surgery. Following [24], we interleave **Convolutional Neck** blocks after the 3rd, 6th, 9th, and 12th transformer blocks. These convolutional injections re-introduce

high-frequency signals—such as tissue grain and vessel structures—into the feature stream before they reach the multi-scale decoder.

C. Self-Supervised Optimization

Since dense ground truth is unavailable in clinical settings, we train the network using a view-synthesis objective.

1) *Decoupled Pose and Intrinsic*s: Standard self-supervised methods assume a fixed, known camera calibration. In endoscopic video, focal length varies with zooming. We therefore employ the decoupled Pose-Intrinsic network from [24], which utilizes rotational constraints to disentangle focal length estimation from translation, preventing the degeneracy common in joint estimation.

2) *Loss Function*: The network is optimized by minimizing the photometric reconstruction error between a target frame I_t and a source frame I_s warped into the target view ($I_{s \rightarrow t}$). We utilize the standard combination of Structural Similarity (SSIM) and L1 difference:

$$L_p = \alpha \frac{1 - \text{SSIM}(I_t, I_{s \rightarrow t})}{2} + (1 - \alpha) |I_t - I_{s \rightarrow t}|. \quad (2)$$

We further apply an edge-aware smoothness loss L_e [25] to discourage artifacts in textureless regions. The final objective is a weighted sum: $L_{total} = L_p + \lambda L_e$.

IV. EXPERIMENTS

A. Dataset and Evaluation Protocol

We validate our framework on the **SCARED** dataset [14], a standard benchmark for endoscopic depth estimation featuring fresh porcine cadaver anatomy captured with a da Vinci Xi robot.

1) *Physically-Stratified Protocol (Hypothesis 1)*: Standard evaluation metrics often average performance across all pixels, masking failures in critical regions. As noted in [8], structured light sensors frequently fail in areas of high specular reflection (common on wet tissue), resulting in "invalid" pixels in the ground truth. To rigorously assess robustness, we introduce a physically-stratified protocol. We use a Gaussian Mixture Model (GMM) to unsupervisedly cluster test frames based on the density of valid ground truth pixels. This yields three regimes: **Hard** (High Specularity, Cluster 1, $\approx 20\%$ valid), **Medium** (Cluster 0), and **Easy** (Cluster 2, $\approx 53\%$ valid).

B. Results

1) *Comparison with State-of-the-Art*: Table I compares our method against established self-supervised baselines. On the aggregate test set, our framework achieves state-of-the-art accuracy, outperforming the strongest V1-based baseline (EndoDAC) and significantly surpassing traditional methods.

2) *Robustness Analysis (Stratified Evaluation)*: The benefits of Synthetic Priors become evident when analyzing the physically-stratified results (Table II). In the **Hard (Specular)** cluster, our V2-based model outperforms the V1 baseline, specifically reducing the Squared Relative Error from 0.341 to 0.325. This confirms that the synthetic pre-training allows

the model to "see through" specular highlights that confuse real-world trained models. Figure 1 qualitatively demonstrates this advantage.

3) *Performance on Baseline Failure Modes*: To further analyze the improvements, we stratified the test set based on the error distribution of the baseline V1 model (Hypothesis 2). As shown in Table III, in frames where the V1 baseline fails significantly ("Hard", $\mu_{error} \approx 0.088$), our V2-based approach reduces the Squared Relative Error from 0.864 to 0.819 and RMSE from 7.152 to 6.893. This suggests that the Synthetic Priors effectively correct the specific failure modes (e.g., outliers and gross artifacts) inherent to real-world trained backbones.

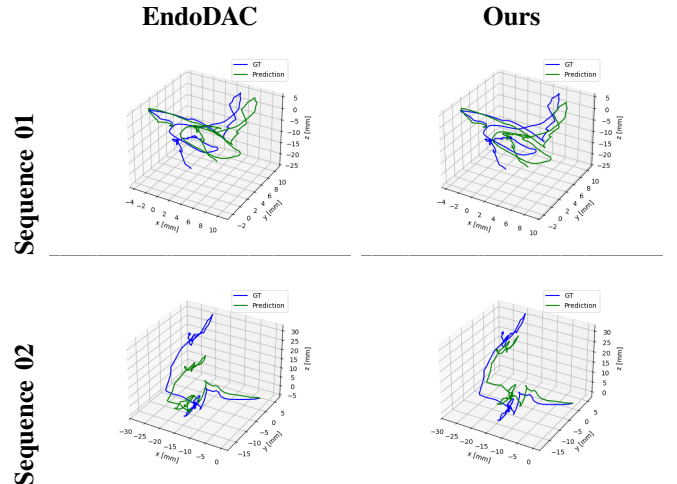


Fig. 3. Qualitative pose estimation comparison on the SCARED dataset. The rows correspond to Sequence 01 and Sequence 02. Our method (Right) significantly reduces trajectory drift compared to the baseline (Left), maintaining tighter alignment with the Ground Truth (Blue).

V. CONCLUSION

In this work, we presented a robust framework for endoscopic monocular depth estimation that addresses the critical challenge of **adverse illumination conditions** in robotic surgery. By identifying the limitations of real-world self-supervision—specifically the "label noise" that obscures thin surgical tools—we proposed a paradigm shift toward leveraging **synthetic priors**. Through the efficient integration of the *Depth Anything V2* backbone with Dynamic Vector LoRA, we successfully transferred precise geometric representations from synthetic environments to the surgical domain. Furthermore, our introduction of a **physically-stratified evaluation protocol** on the SCARED dataset provides a more rigorous benchmark for the field. Experimental results demonstrate that our approach achieves state-of-the-art accuracy and significantly outperforms baselines in challenging, specular-dominant scenes.

ACKNOWLEDGMENTS

This research was partially funded by the NIH under grant number 1R15EB034519-01A1 and NSF under grant number 2346790.

TABLE I
 QUANTITATIVE COMPARISON OF STATE-OF-THE-ART METHODS ON THE SCARED DATASET.

Method	Abs Rel ↓	Sq Rel ↓	RMSE ↓	RMSE _{log} ↓	$\delta < 1.25$ ↑
SC-SfMLearner [26]	0.068	0.645	5.988	0.097	0.957
Monodepth2 [27]	0.069	0.577	5.546	0.094	0.948
[28]	0.078	0.794	6.794	0.109	0.946
Defeat-Net [29]	0.077	0.792	6.688	0.108	0.941
Endo-SfM [30]	0.062	0.606	5.726	0.093	0.957
AF-SfMLearner [31]	0.059	0.435	4.925	0.082	0.974
[32]	0.062	0.558	5.585	0.090	0.962
DA (zero-shot) [21]	0.084	0.847	6.711	0.110	0.930
DA (fine-tuned)	0.058	0.451	5.058	0.081	0.974
EndoDAC [24]	0.052	0.370	4.582	0.074	0.976
Our	0.051	0.360	4.527	0.073	0.981

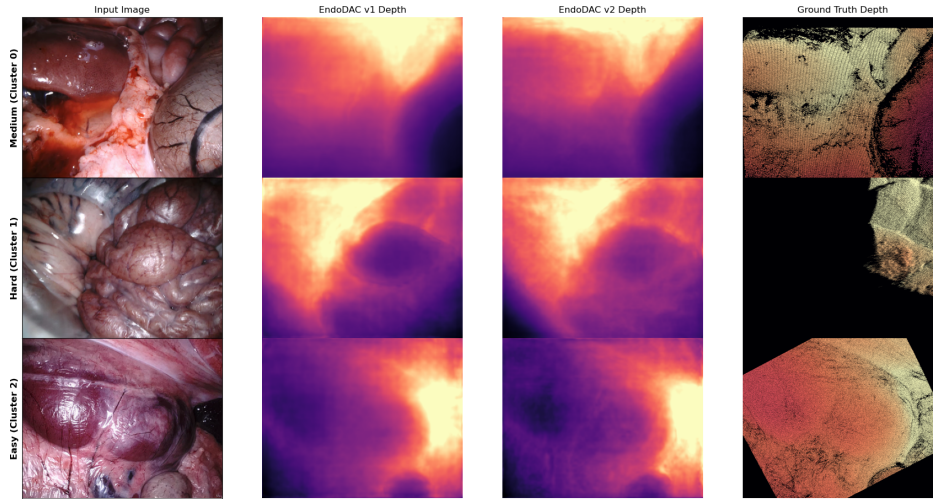


Fig. 1. Qualitative comparison (Hypothesis 1) across difficulty clusters. The rows correspond to Medium (Top), Hard (Middle), and Easy (Bottom) subsets.

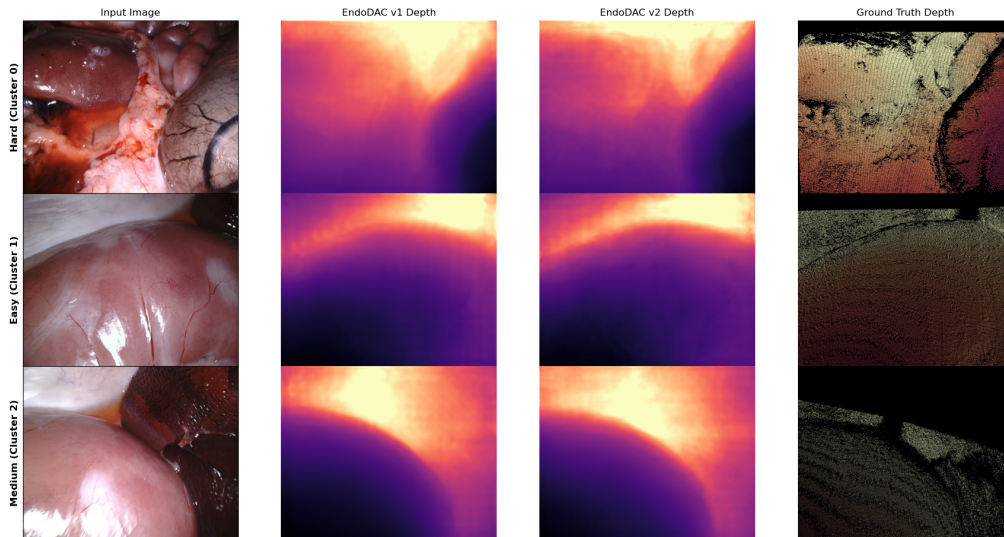


Fig. 2. Qualitative comparison (Hypothesis 2) across difficulty clusters. The rows correspond to Hard (Top), Easy (Middle), and Medium (Bottom) subsets.

TABLE II

PHYSICALLY-STRATIFIED QUANTITATIVE COMPARISON (HYPOTHESIS 1). GROUPING BY DIFFICULTY REVEALS THAT OUR METHOD OUTPERFORMS THE V1 BASELINE IN THE **HARD** AND **MEDIUM** CATEGORIES, WHICH REPRESENT THE MAJORITY OF THE DATASET (475/551 FRAMES).

Method	Abs Rel (\downarrow)	Sq Rel (\downarrow)	RMSE (\downarrow)	RMSE _{log} (\downarrow)	$\delta < 1.25$ (\uparrow)	
Hard (Cluster 1, $N = 301$)	V1	0.046	0.341	4.390	0.069	0.980
	V2 (Ours)	0.045	0.325	4.293	0.067	0.983
Easy (Cluster 2, $N = 76$)	V1	0.058	0.400	5.236	0.078	0.977
	V2 (Ours)	0.059	0.424	5.473	0.079	0.982
Medium (Cluster 0, $N = 174$)	V1	0.058	0.406	4.623	0.081	0.969
	V2 (Ours)	0.059	0.391	4.517	0.079	0.977

TABLE III

PERFORMANCE ON BASELINE FAILURE MODES (HYPOTHESIS 2). FRAMES ARE CLUSTERED BY THE ERROR MAGNITUDE OF THE V1 BASELINE. OUR METHOD SHOWS SIGNIFICANT RECOVERY IN THE "HARD" CLUSTER, INDICATING IT FIXES SPECIFIC V1 FAILURE CASES.

Difficulty	Model	Abs Rel	Sq Rel	RMSE	RMSE _{log}	$\delta < 1.25$
Hard (Cluster 0, $N = 71$)	V1	0.094	0.864	7.152	0.129	0.921
	V2 (Ours)	0.091	0.819	6.893	0.125	0.935
Easy (Cluster 1, $N = 283$)	V1	0.035	0.181	3.415	0.051	0.995
	V2 (Ours)	0.036	0.195	3.495	0.051	0.995
Medium (Cluster 2, $N = 197$)	V1	0.060	0.462	5.328	0.088	0.970
	V2 (Ours)	0.059	0.431	5.156	0.084	0.978

REFERENCES

- [1] Y. Lin, J. Tremblay, S. Tyree, P. A. Vela, and S. Birchfield, "Multi-view fusion for multi-level robotic scene understanding," in *2021 IEEE/RSJ International Conference on Intelligent Robots and Systems (IROS)*. IEEE, 2021, pp. 6817–6824.
- [2] Y. Li and B. Hannaford, "Gaussian process regression for sensorless grip force estimation of cable-driven elongated surgical instruments," *IEEE Robotics and Automation Letters*, vol. 2, no. 3, pp. 1312–1319, 2017.
- [3] T. Mane, A. Bayramova, K. Daniilidis, P. Mordohai, and E. Bernardis, "Single-camera 3d head fitting for mixed reality clinical applications," *Computer Vision and Image Understanding*, vol. 218, p. 103384, 2022.
- [4] Y. Li, N. Konuthula, I. M. Humphreys, K. Moe, B. Hannaford, and R. Bly, "Real-time virtual intraoperative ct in endoscopic sinus surgery," *International Journal of Computer Assisted Radiology and Surgery*, pp. 1–12, 2022.
- [5] Y. Tian, Y. Chang, F. H. Arias, C. Nieto-Granda, J. P. How, and L. Carlone, "Kimera-multi: Robust, distributed, dense metric-semantic slam for multi-robot systems," *IEEE Transactions on Robotics*, vol. 38, no. 4, 2022.
- [6] P. R. Florence, L. Manuelli, and R. Tedrake, "Dense object nets: Learning dense visual object descriptors by and for robotic manipulation," *arXiv preprint arXiv:1806.08756*, 2018.
- [7] Y. Li, R. Bly, S. Akkina, F. Qin, R. C. Saxena, I. Humphreys, M. Whipple, K. Moe, and B. Hannaford, "Learning surgical motion pattern from small data in endoscopic sinus and skull base surgeries," in *2021 IEEE International Conference on Robotics and Automation (ICRA)*. IEEE, 2021, pp. 7751–7757.
- [8] Y. Lee, "Three-dimensional dense reconstruction: A review of algorithms and datasets," *Sensors*, vol. 24, no. 18, p. 5861, 2024.
- [9] Y. Li, S. Li, and Y. Ge, "A biologically inspired solution to simultaneous localization and consistent mapping in dynamic environments," *Neurocomputing*, vol. 104, pp. 170–179, 2013.
- [10] J. Lamarca, S. Parashar, A. Bartoli, and J. Montiel, "Defslam: Tracking and mapping of deforming scenes from monocular sequences," *IEEE Transactions on robotics*, vol. 37, no. 1, pp. 291–303, 2020.
- [11] Y. Li and B. Hannaford, "Soft-obstacle avoidance for redundant manipulators with recurrent neural network," in *Intelligent Robots and Systems (IROS), 2018 IEEE/RSJ International Conference on*. IEEE, 2018, pp. 1–6.
- [12] N. Mahmoud, I. Cirauqui, A. Hostettler, C. Doignon, L. Soler, J. Marescaux, and J. Montiel, "Orbslam-based endoscope tracking and 3d reconstruction," in *International workshop on computer-assisted and robotic endoscopy*. Springer, 2016, pp. 72–83.
- [13] T. Okatani and K. Deguchi, "Shape reconstruction from an endoscope image by shape from shading technique for a point light source at the projection center," *Computer vision and image understanding*, vol. 66, no. 2, pp. 119–131, 1997.
- [14] M. Allan, J. Mcleod, C. Wang, J. C. Rosenthal, Z. Hu, N. Gard, P. Eisert, K. X. Fu, T. Zeffiro, W. Xia *et al.*, "Stereo correspondence and reconstruction of endoscopic data challenge," *arXiv preprint arXiv:2101.01133*, 2021.
- [15] S. Shao, Z. Pei, W. Chen, W. Zhu, X. Wu, D. Sun, and B. Zhang, "Self-supervised monocular depth and ego-motion estimation in endoscopy: Appearance flow to the rescue," *arXiv preprint arXiv:2112.08122*, 2021.
- [16] A. Vaswani, "Attention is all you need," *Advances in Neural Information Processing Systems*, 2017.
- [17] B. Mildenhall, P. P. Srinivasan, M. Tancik, J. T. Barron, R. Ramamoorthi, and R. Ng, "Nerf: Representing scenes as neural radiance fields for view synthesis," *Communications of the ACM*, vol. 65, no. 1, pp. 99–106, 2021.
- [18] B. Kerbl, G. Kopanas, T. Leimkühler, and G. Drettakis, "3d gaussian splatting for real-time radiance field rendering," *ACM Trans. Graph.*, vol. 42, no. 4, pp. 139–1, 2023.
- [19] J. Ho, A. Jain, and P. Abbeel, "Dennoising diffusion probabilistic models," *Advances in neural information processing systems*, vol. 33, pp. 6840–6851, 2020.
- [20] A. Kirillov, E. Mintun, N. Ravi, H. Mao, C. Rolland, L. Gustafson, T. Xiao, S. Whitehead, A. C. Berg, W.-Y. Lo *et al.*, "Segment anything," in *Proceedings of the IEEE/CVF international conference on computer vision*, 2023, pp. 4015–4026.
- [21] L. Yang, B. Kang, Z. Huang, X. Xu, J. Feng, and H. Zhao, "Depth anything: Unleashing the power of large-scale unlabeled data," in *CVPR*, 2024.
- [22] F. Remondino, A. Karami, Z. Yan, G. Mazzacca, S. Rigon, and R. Qin, "A critical analysis of nerf-based 3d reconstruction," *Remote Sensing*, vol. 15, no. 14, p. 3585, 2023.
- [23] L. Yang, B. Kang, Z. Huang, Z. Zhao, X. Xu, J. Feng, and H. Zhao, "Depth anything v2," *arXiv:2406.09414*, 2024.
- [24] B. Cui, M. Islam, L. Bai, A. Wang, and H. Ren, "Endodac: Efficient adapting foundation model for self-supervised depth estimation from any endoscopic camera," *arXiv*, 2024.
- [25] C. Godard, O. M. Aodha, M. Firman, and G. J. Brostow, "Digging into self-supervised monocular depth estimation," in *Proceedings of the IEEE/CVF International Conference on Computer Vision*, 2019, pp. 3828–3838.

- [26] J. Bian, Z. Li, N. Wang, H. Zhan, C. Shen, M.-M. Cheng, and I. Reid, "Unsupervised scale-consistent depth and ego-motion learning from monocular video," *Advances in neural information processing systems*, vol. 32, 2019.
- [27] C. Godard, O. Mac Aodha, M. Firman, and G. J. Brostow, "Digging into self-supervised monocular depth estimation," in *Proceedings of the IEEE/CVF International Conference on Computer Vision*, 2019, pp. 3828–3838.
- [28] Z. Fang, X. Chen, Y. Chen, and L. V. Gool, "Towards good practice for cnn-based monocular depth estimation," in *Proceedings of the IEEE/CVF winter conference on applications of computer vision*, 2020, pp. 1091–1100.
- [29] J. Spencer, R. Bowden, and S. Hadfield, "Defeat-net: General monocular depth via simultaneous unsupervised representation learning," in *Proceedings of the IEEE/CVF conference on computer vision and pattern recognition*, 2020, pp. 14 402–14 413.
- [30] K. B. Ozyoruk, G. I. Gokceler, T. L. Bobrow, G. Coskun, K. Incetan, Y. Almalioglu, F. Mahmood, E. Curto, L. Perdigoto, M. Oliveira *et al.*, "Endoslam dataset and an unsupervised monocular visual odometry and depth estimation approach for endoscopic videos," *Medical image analysis*, vol. 71, p. 102058, 2021.
- [31] S. Shao, Z. Pei, W. Chen, W. Zhu, X. Wu, D. Sun, and B. Zhang, "Self-supervised monocular depth and ego-motion estimation in endoscopy: Appearance flow to the rescue," *Medical image analysis*, vol. 77, p. 102338, 2022.
- [32] Z. Yang, J. Pan, J. Dai, Z. Sun, and Y. Xiao, "Self-supervised lightweight depth estimation in endoscopy combining cnn and transformer," *IEEE Transactions on Medical Imaging*, vol. 43, no. 5, pp. 1934–1944, 2024.